The Journal of Chemical Physics

Intermolecular interactions in optical cavities: An *ab initio* QED study

Cite as: J. Chem. Phys. **154**, 094113 (2021); https://doi.org/10.1063/5.0039256
Submitted: 02 December 2020 . Accepted: 05 February 2021 . Published Online: 02 March 2021

Tor S. Haugland, Christian Schäfer, Enrico Ronca, Angel Rubio, and Henrik Koch

AIP Publishing

The Journal of Chemical Physics ARTICLE scitation.org/journal/jcp

Intermolecular interactions in optical cavities: An *ab initio* QED study

Cite as: J. Chem. Phys. 154, 094113 (2021); doi: 10.1063/5.0039256
Submitted: 2 December 2020 • Accepted: 5 February 2021 •
Published Online: 2 March 2021

Tor S. Haugland,[1] Christian Schäfer,[2] Enrico Ronca,[2,3] Angel Rubio,[2,4,5] and Henrik Koch[1,6,a)]

AFFILIATIONS

[1] Department of Chemistry, Norwegian University of Science and Technology, 7491 Trondheim, Norway
[2] Max Planck Institute for the Structure and Dynamics of Matter and Center Free-Electron Laser Science, Luruper Chaussee 149, 22761 Hamburg, Germany
[3] Istituto per i Processi Chimico Fisici del CNR (IPCF-CNR), Via G. Moruzzi, 1, 56124 Pisa, Italy
[4] Center for Computational Quantum Physics (CCQ), The Flatiron Institute, 162 Fifth Avenue, New York, New York 10010, USA
[5] Nano-Bio Spectroscopy Group, Departamento de Física de Materiales, Universidad del País Vasco, 20018 San Sebastian, Spain
[6] Scuola Normale Superiore, Piazza dei Cavalieri, 7, 56124 Pisa, Italy

Note: This paper is part of the JCP Special Topic on Polariton Chemistry: Molecules in Cavities and Plasmonic Media.
[a)] **Author to whom correspondence should be addressed:** henrik.koch@sns.it

ABSTRACT

Intermolecular bonds are weak compared to covalent bonds, but they are strong enough to influence the properties of large molecular systems. In this work, we investigate how strong light–matter coupling inside an optical cavity can modify intermolecular forces and illustrate the varying necessity of correlation in their description. The electromagnetic field inside the cavity can modulate the ground state properties of weakly bound complexes. Tuning the field polarization and cavity frequency, the interactions can be stabilized or destabilized, and electron densities, dipole moments, and polarizabilities can be altered. We demonstrate that electron–photon correlation is fundamental to describe intermolecular interactions in strong light–matter coupling. This work proposes optical cavities as a novel tool to manipulate and control ground state properties, solvent effects, and intermolecular interactions for molecules and materials.

I. INTRODUCTION

Intermolecular interactions play a fundamental role in chemistry and physics, and they are especially important in describing the properties of large systems. In particular, they contribute to solvation processes,[1] interactions in liquids,[2] gas phase reactivity,[3] formation of higher order structures in biological macromolecules,[4] and multi-layer 2D materials.[5–8] The ability to induce even minor modifications in the intermolecular forces can have a large impact on the macroscopic properties of molecular systems. In this respect, strong light–matter coupling is an exciting possibility for changing weak interactions.

Over the last decade, strong light–matter coupling via optical cavities has been unveiled as a new tool that can modify molecular properties and interactions in a non-intrusive manner. Recent seminal experimental works have demonstrated the possibility to inhibit,[9–11] steer,[12] and accelerate[13–16] chemical reactions by strong light–matter coupling inside micro-[17,18] and plasmonic[19,20] cavities. Furthermore, cavities have been applied to enhance charge and energy transfer,[21–27] design materials,[28] and control superconductivity.[29–31]

From a theoretical point of view, strong light–matter coupling has been extensively investigated since the 1950s using simplified descriptions of the electronic system.[32–34] Using model Hamiltonians, a broad range of fascinating insight has been achieved. However, connecting these predictions to experimental observations in polaritonic chemistry is quite challenging.[36–39] The models typically account for the main features of strong light–matter coupling, such

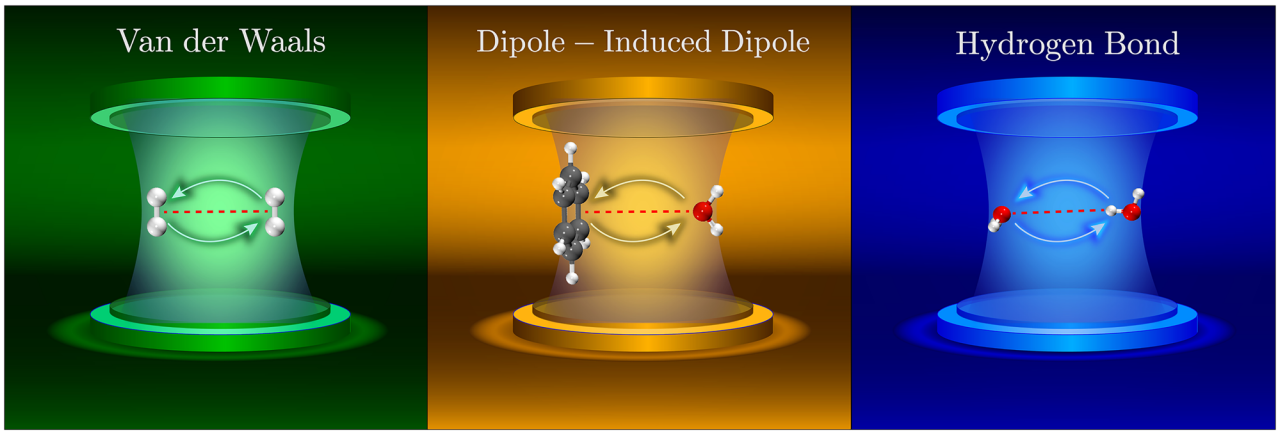

FIG. 1. Main intermolecular interactions, here in optical cavities.

as Rabi splittings,[40] but are unable to quantitatively capture changes in molecular systems. In situations where the coupling between light and matter is of the same magnitude as other interactions, for instance, intermolecular forces, the simplified models are not sufficient. In order to achieve accuracy in chemical predictions, the full complexity of the system must be considered. Quantum electrodynamical density functional theory (QEDFT)[41] and quantum electrodynamics coupled cluster theory (QED-CC)[42] are *ab initio* methodologies that accurately model correlated electron–photon systems. Recent applications of these methods include calculation of cavity-induced changes in the ground state,[43,44] ionization energies,[45] and local polaritonic effects.[46]

In this paper, we employ QEDFT and QED-CC to study intermolecular forces under the influence of strong light–matter coupling. We have selected three systems as examples of van der Waals interaction, dipole-induced dipole interaction, and hydrogen bonding (see Fig. 1). Benchmark calculations are performed using the QED full configuration interaction (QED-FCI) method wherever possible. For the hydrogen bonded system, we analyze changes in the electron density and investigate the long-range interaction through the cavity field. Only the ground state of the light–matter systems is investigated. We note that dispersion interaction in DFT is a particularly complicated problem[47] even without any cavity environment. Nevertheless, QEDFT represents the only *ab initio* alternative to QED-CC. For this reason, showing a comparison is interesting as we focus on cavity-induced effects.

This paper is organized as follows. In Sec. II, we introduce the computational approaches. Section III presents our investigation of cavity-induced effects on intermolecular interactions. Section IV contains our concluding remarks.

II. COMPUTATIONAL APPROACHES

In nonrelativistic QED, the interaction between molecules and quantized electromagnetic fields is described by the Pauli–Fierz Hamiltonian.[48,49] For a single photon mode in the dipole approximation, the time-independent Hamiltonian in Coulomb gauge and after subsequent Power–Zienau–Woolley transformation[50,51] reads

$$H_e = -\frac{1}{2}\sum_i^{N_e}\nabla_i^2 - \sum_i^{N_e}\sum_I^{N_{\mathrm{nuc}}}\frac{Z_I}{|\boldsymbol{r}_i - \boldsymbol{R}_I|} + \frac{1}{2}\sum_{i\neq j}^{N_e}\frac{1}{|\boldsymbol{r}_i - \boldsymbol{r}_j|} + \frac{1}{2}\sum_{I\neq J}^{N_{\mathrm{nuc}}}\frac{Z_I Z_J}{|\boldsymbol{R}_I - \boldsymbol{R}_J|}, \tag{1}$$

$$H = H_e + \omega b^\dagger b + \lambda\sqrt{\frac{\omega}{2}}(\boldsymbol{\varepsilon}\cdot\Delta\boldsymbol{d})(b + b^\dagger) + \frac{\lambda^2}{2}(\boldsymbol{\varepsilon}\cdot\Delta\boldsymbol{d})^2. \tag{2}$$

Here, H_e is the electronic Hamiltonian in the Born–Oppenheimer approximation in standard notation. The second term of Eq. (2) is the photon contribution to the energy, where ω is the photon mode frequency and $b/b^\dagger$ are the associated annihilation/creation operators. The third term is the bilinear light–matter interaction and depends on the fluctuations of the molecular dipole, $\Delta\boldsymbol{d} = \boldsymbol{d} - \langle\boldsymbol{d}\rangle$, and the field transversal polarization vector $\boldsymbol{\varepsilon}$. The coupling strength λ is determined by the quantization volume V, $\lambda = \sqrt{4\pi/V}$. The last term is the dipole self-energy (DSE) that describes the molecular self-interaction through the field and further ensures that the total Hamiltonian is gauge and origin invariant, and bound from below.[42,51] Light–matter coupling introduces interesting features into the quantum chemical picture. Even for very large distances, molecules can still interact through the cavity photons[25] and the total energy is not size-extensive, as is the case without the cavity environment.

In quantum chemistry, there are two main approaches to solve the electronic Schrödinger equation: wave function theory[52] and density functional theory.[53] To solve the eigenvalue problem for the light–matter Hamiltonian [Eq. (2)], the photons must be treated on the same level of quantization as the electrons. For this reason, only a few molecular approaches have been extended to quantum electrodynamics. Only recently, extensions of DFT, Hartree–Fock (HF), CC, and FCI became available to perform *ab initio* simulations of strong light–matter coupling. In Secs. II A and II B, we give a brief introduction to these methodologies.

A. QED wave function approaches

Hartree–Fock theory (HF), which employs a single Slater determinant, is the usual starting point for developing approximate wave function methods. This approach does not include any electron correlation. One of the most successful and accurate methods to include correlation is coupled cluster theory, which includes additional determinants through an exponential parameterization starting from the HF wave function.[52]

In Hartree–Fock theory, the photonic degrees of freedom are included by treating the electrons and photons as uncorrelated particles interacting through a mean-field potential. This leads to the formulation of quantum electrodynamics Hartree–Fock theory (QED-HF).[42] Similarly to coupled cluster theory for electrons, QED-HF is the starting point for QED-CC.[42] The correlated QED-CC wave function is expressed as

$$|\mathrm{CC}\rangle = \exp(T)|R\rangle, \tag{3}$$

where $|R\rangle = |\mathrm{HF}\rangle \otimes |0\rangle$ is the QED-HF state. Here, T is the cluster operator,

$$T = \sum_{\mu n} t_\mu^n \tau_\mu (b^\dagger)^n, \tag{4}$$

and t_μ^n are the amplitudes for the electronic determinant $|\mu\rangle$ and photon occupation $|n\rangle$, and $\tau_\mu(b^\dagger)^n$ is the corresponding excitation operator,

$$\tau_\mu (b^\dagger)^n |R\rangle = |\mu\rangle \otimes |n\rangle \sqrt{(n+1)!}. \tag{5}$$

The QED-CC formulation is exact in the limit where all electronic and photonic states are included. In practice, because of the infinite number of states, a truncation must be introduced. In this paper, we consider QED-CCSD-1, which employs a cluster operator

$$T = T_1 + T_2 + S_1^1 + S_2^1 + \Gamma^1, \tag{6}$$

where T_1 and T_2 are linear combinations of electronic single and double excitations, S_1^1 and S_2^1 are electronic single and double excitations coupled with a single photon creation, and Γ^1 is the single photon creation operator. The QED-CCSD-1 scales as N^6 with respect to the number of electronic basis functions, and it is computationally feasible for medium sized molecules.

If no truncation of the excitation operators is performed, QED-CC is equivalent to the exact treatment of QED-FCI. However, implementing QED-FCI in a coupled cluster formulation is inconvenient. For this reason, we use a direct determinant-based CI implementation[52] to diagonalize the Hamiltonian in Eq. (2) in the direct product basis of electronic determinants and photon number states.

All the mentioned wave function methods are implemented and calculated using the e^T-program.[54]

B. QED density functional theory

Quantum electrodynamical density functional theory is based on the key observation of ordinary DFT that all observables relevant in electronic structure theory are functionals of the electronic density $n(\mathbf{r})$. Density functional theory uses the unique relation between the electronic density and external potential[55] to set up and solve a set of single-particle Kohn–Sham equations.[56] The occupied orbitals $\varphi_i(\boldsymbol{r})$ fulfill

$$\left[-\frac{1}{2}\nabla^2 + v_s(\boldsymbol{r})\right]\varphi_i(\boldsymbol{r}) = \epsilon_i \varphi_i(\boldsymbol{r}) \tag{7}$$

and provide the exact electronic density

$$n(\mathbf{r}) = \sum_i |\varphi_i(\boldsymbol{r})|^2 \tag{8}$$

associated with the potential

$$v_s(\boldsymbol{r}) = v_{ext}(\boldsymbol{r}) + v_H(\boldsymbol{r}) + v_{xc}(\boldsymbol{r}). \tag{9}$$

This local Kohn–Sham potential is characterized by the known external and classical Hartree potentials as well as the unknown exchange-correlation potential $v_{xc}(\boldsymbol{r})$. Naturally, $v_{xc}(\boldsymbol{r})$ is known only approximately and DFT is (in practice) often accurate and computationally efficient but never exact.

The QEDFT approach extends this idea to quantum electrodynamics.[41] Through the formulation of effective single-particle Kohn–Sham and Maxwell equations, QEDFT reproduces the exact many-body problem if the exact functionals for the electron–electron and electron–photon interactions are known. In this paper, we utilize the optimized effective potential (OEP) approach[43,57,58] to obtain the exact-exchange potential

$$v_{xc}(\mathbf{r}) \approx v_x^{\mathrm{OEP,Coulomb}}(\mathbf{r}) + v_x^{\mathrm{OEP,photons}}(\mathbf{r}) \tag{10}$$

for both the Coulomb and photonic interactions. The latter is the variational derivative

$$v_x^{\mathrm{OEP,photons}}(\mathbf{r}) = \delta E_x^{\mathrm{photons}} / \delta n(\mathbf{r}) \tag{11}$$

of the self-consistent second-order correction to the energy[43,58]

$$E_x^{\mathrm{photons}} = \frac{1}{2}\lambda^2 \sum_{a,i} |\langle \varphi_a | \boldsymbol{\varepsilon}\cdot\boldsymbol{d} | \varphi_i \rangle|^2 \left(1 - \frac{\omega}{\epsilon_a - \epsilon_i + \omega}\right), \tag{12}$$

where a labels the unoccupied Kohn–Sham orbitals. Using density-functional perturbation theory, the density dependence of the Kohn–Sham orbitals leads to coupled Sternheimer (coupled perturbed Kohn–Sham) equations that are solved self-consistently.[43,59]

The combination of QEDFT and the OEP functional (QEDFT/OEP) gives rise to an exact-exchange treatment of the electronic structure in the presence of the cavity. In this way, it describes the interaction of electrons on a similar but not equivalent level as Hartree–Fock.[57] In contrast to QED-HF, the QEDFT/OEP solution features also electronic exchange mediated by the photonic fluctuations in addition to the exchange originating from the DSE. For the systems investigated here, the correct long-range $1/r$ decay is an especially desirable feature of the OEP that is not common to all possible realizations of DFT. QEDFT itself is a much more versatile concept than the here selected OEP approach and correlation functionals are currently in development.

All reported calculations have been performed with the OCTOPUS code[59] using the standard Troullier–Martins pseudopotentials, a Cartesian grid, and eighth-order finite differences.

III. RESULTS

Covalent bonds between valence electrons typically have binding energies of about 1 eV–10 eV. Intermolecular bonds are

substantially weaker (1 meV–300 meV), and they arise from van der Waals interaction or electrostatics (dipole–dipole, etc.).[60] Even though their strength is orders of magnitude weaker than covalent and ionic bonds, they are not negligible. Intermolecular forces can also be interpreted in terms of electron interactions mediated by the transverse electromagnetic field.[61] Because of this parallelism, changing the boundary conditions of the field with a cavity will alter the interactions.[62–64]

In this paper, we treat a single effective cavity mode interacting explicitly with the molecular system and assume that the electron mass inside the cavity is the same as outside.[61,65] For non-correlated QED-HF, multi-mode calculations are equivalent to replacing the coupling with an effective coupling that is the norm of all the mode parameters, $\lambda_{\text{eff}}^2 = \sum_n \lambda_n^2$ (assuming the same polarization). In the correlated approaches considered here, we approximate the multi-mode scenario by using a single effective mode with $\lambda = 0.1$. This is larger than what has been experimentally realized for a single mode.[66] We justify the enlarged coupling by the many additional modes available in experiments. This description is certainly limited, and going beyond this will require more sophisticated considerations from the photonic point of view. However, new insight into a non-perturbative description of cavity mediated weak interactions can be obtained using this approximation. By explicitly varying λ and ω, the results were little affected. Reducing the coupling strength reduced the magnitude of the here illustrated effects, and changing the frequency around the electronic excitation energy shows minor effect. When tuning the frequency, one effectively tunes the size of the bilinear interaction relative to the dipole self-energy.[51] The frequency dispersion is shown in the supplementary material. We conclude that our investigation remains relevant for a variety of cavity realizations. Cavity losses, which only lead to quantitative and not qualitative changes of the results, are neglected in this paper.[67]

In the following, cavity-induced effects on the different kinds of intermolecular interactions are discussed. These cases range from weak to strong intermolecular forces.

A. van der Waals interaction

The weakest among the intermolecular interactions is van der Waals (vdW),[60] characterized by energies of about 1 meV–50 meV. Usually, they are described as interactions between the polarizabilities of the constituent fragments A and B through the London formula,[68]

$$V_{\text{London}} = -\frac{3}{2}\left(\frac{I_A I_B}{I_A + I_B}\right)\frac{\tilde{\alpha}_A \tilde{\alpha}_B}{R^6}, \tag{13}$$

where I_A is the ionization energy of system A, $\tilde{\alpha}_A$ is the mean polarizability of A, and R is the distance between the fragments. This approximation neglects retardation effects appearing at long distances that modify the scaling to R^{-7}.[61] The polarizability is closely related to dipole fluctuations by the relation

$$\alpha_{\gamma\gamma} = 2\sum_{n\neq 0}\frac{\langle\psi_0|d_\gamma|\psi_n\rangle\langle\psi_n|d_\gamma|\psi_0\rangle}{E_n - E_0} \approx \frac{2\langle\Delta d_\gamma^2\rangle}{I}, \tag{14}$$

where $\gamma \in \{x, y, z\}$. Inserting Eq. (14) into the London formula in Eq. (13), evident similarities with the dipole self-energy

$$E_{DSE} = \frac{1}{2}\lambda^2\langle(\boldsymbol{\varepsilon}\cdot\Delta\boldsymbol{d})^2\rangle \tag{15}$$

can be observed. The London formula can also be derived from the bilinear light–matter interaction between the fragments in free space.[61]

Cavity-induced effects will be analyzed for the $(H_2)_2$ complex. Three polarization directions (ε) are considered, and the cavity frequency is set in resonance with the first coupled cluster singles and doubles (CCSD) excited state of H_2, $\omega = 12.7$ eV. The wave function calculations are performed with an aug-cc-pVDZ orbital basis with a bond distance of 0.74 Å. The DFT/OEP and QEDFT/OEP results are obtained using a spherical grid centered around each atom with radius 14 and spacing 0.25 a_0, and the H_2 bond distance was optimized using the KLI functional obtaining 0.73 Å.

In Fig. 2, we compare the potential energy curves calculated with CCSD/QED-CCSD-1 and FCI/QED-FCI. Field polarizations along the H_2 bond (ε_x) and chain axis (ε_z) are presented here. The other orthogonal polarization (ε_y), being qualitatively similar to ε_x, is shown in the supplementary material for completeness. In this study, QED-FCI results are converged with the number of photons.

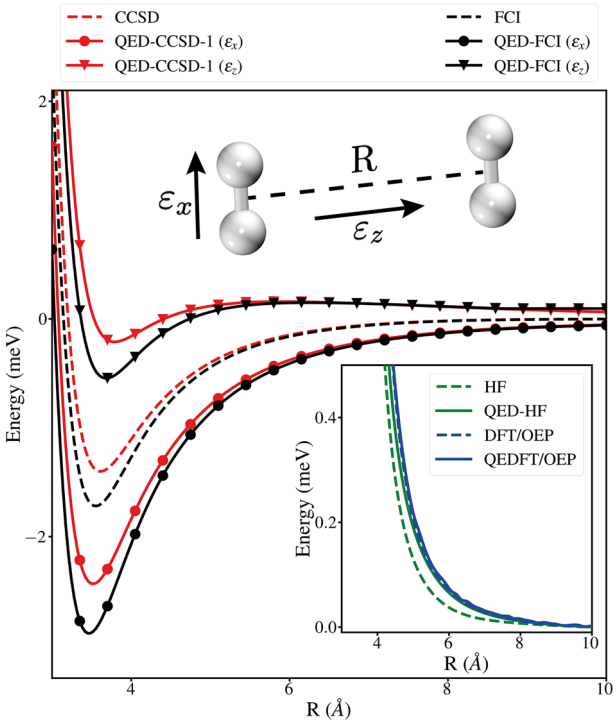

FIG. 2. Potential energy curves calculated for $(H_2)_2$ outside (dashed line) and inside a cavity with $\lambda = 0.1$ and $\omega = 12.7$ eV, with different markers for the different polarizations. For each curve, the energy at 200 Å has been subtracted. The inset shows the same curves for non-correlated methods with field polarization along ε_x.

From Fig. 2, we see that coupled cluster is in good agreement with the reference FCI values, but it slightly underestimates the binding energy. This is the case both outside and inside the cavity for all field polarization directions. This behavior is well known from coupled cluster theory, and it has been extensively discussed in Ref. 52. Including perturbative triples in QED-CC, either with CC3 or with CCSD(T),[69,70] will make the total ground state energy quantitatively more accurate compared to the reference. Similar effects can also be observed for different molecular geometries, as shown in Fig. S3 in the supplementary material.

The Hartree–Fock method, which does not include correlation, is unable to capture the vdW interaction, and the potential energy curves are repulsive, both inside and outside the cavity (see the inset in Fig. 2). This is in contrast to the correlated results. The exchange-only treatment of the OEP functional provides qualitatively similar predictions compared to Hartree–Fock. However, in QEDFT/OEP, the effect of the cavity is minimal as the DSE, bilinear, and photonic contributions to the energy largely compensate each other.

The cavity-induced changes in the potential energy curves are presented in Fig. 3. When the cavity polarization is perpendicular to the intermolecular bond (ε_x and ε_y), the binding energy increases. In contrast, when the field polarization is parallel (ε_z), the cavity destabilizes the bond. Interestingly, the energy difference behaves asymptotically as R^{-3} for large R ($\mathcal{R}^2 > 0.98$, black dashed lines). This is the same dependence as a dipole–dipole interaction instead of the expected R^{-6} behavior of vdW dispersion. In Sec. III D, we show that the interaction between two molecules is independent of distance, and thus, a perturbative treatment should explicitly give the R^{-3} dependence. Outside the cavity, the correlation energy (blue solid line) shows the R^{-6} dependence. Note that the dipole moments of the isolated fragments are zero inside the cavity.

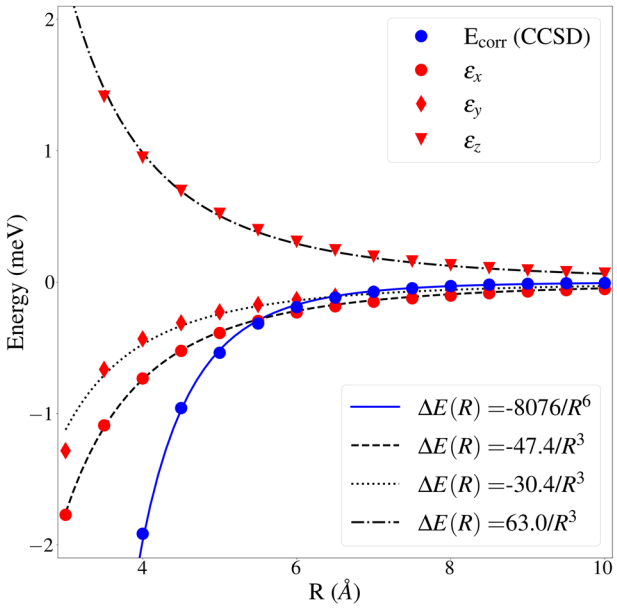

FIG. 3. Correlation energy ($E_{CCSD} - E_{HF}$) and cavity-induced effect on the potential energy curve of $(H_2)_2$ ($E_{QED\text{-}CC} - E_{CC}$) for a cavity with $\lambda = 0.1$ and $\omega = 12.7$ eV. All the fitted curves have $\mathcal{R}^2 > 0.98$.

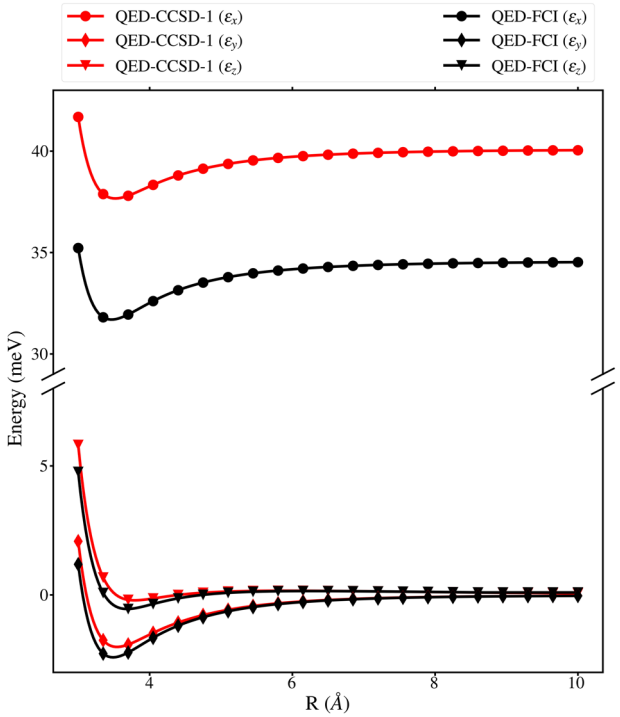

FIG. 4. Potential energy curves calculated with QED-CC and QED-FCI for $(H_2)_2$ inside a cavity with $\lambda = 0.1$ and $\omega = 12.7$ eV, with different markers for the different polarizations. The energy of ε_y at 200 Å has been subtracted.

Figures 2 and 3 show cavity-induced changes in the binding energies, but they do not give any insight into the absolute stability of the system. This is instead found from the relative energy differences (see Fig. 4). The increase in energy due to the dipole self-energy is substantially higher when the polarization is along the H_2 bond (ε_x) compared to the orthogonal field polarizations (ε_y and ε_z). This is because the electrons are more diffuse along the bond, allowing for larger dipole fluctuations, see Eq. (15). The energy difference of about 40 meV induces a preferential orientation of the system along the ε_y and ε_z directions. From Fig. 4, we can also observe that QED-CCSD-1 is missing about 5 meV more correlation when the field polarization is along ε_x compared to the other directions. This result is confirmed by the correlation energies calculated at the minima presented in Table I.

As mentioned in the discussion of Fig. 2, the system is mainly polarizable along the H_2 bond (α_{xx}) as shown in Table II. The overall reduced α inside the cavity indicates that the electron density becomes more localized. The reduction is more evident along the direction of the field polarization (see columns of Table II). In this context, the variational minimization of the DSE reduces the dipole fluctuations and consequently the polarizability [see Eq. (14)]. This observation is in line with density localization effects already discussed in Refs. 25, 42, 43, and 65.

TABLE I. Correlation energies ($E_{\text{QED-CC/FCI}} - E_{\text{QED-HF}}$) in eV for $(H_2)_2$ at equilibrium geometry. The values are calculated inside and outside a cavity with coupling $\lambda = 0.1$ and frequency $\omega = 12.7$ eV for different field polarizations ε.

Method	No cavity	ε_x	ε_y	ε_z
QED-CCSD-1	1.9523	2.2400	2.1408	2.1384
QED-FCI	1.9526	2.2461	2.1438	2.1413

The same cavity-induced reduction of the polarizability is observed for an isolated H_2 molecule, see Table III. This implies, using the London formula in Eq. (13), a reduction of the vdW energy. However, as shown in Fig. 2, the cavity can both increase and decrease the binding energy depending on the field polarization. This result clearly demonstrates that the London formula, as it is usually presented, does not hold for molecules in cavities.[62,71] Note that not only the polarizability is affected by the cavity, but also the ionization energy as recently shown in Ref. 45.

B. Dipole-induced dipole interactions

In this section, the dipole–induced dipole interaction between a polar and a non-polar molecule is analyzed. The dipole induces a charge fluctuation in the other system (induced dipole) that can form an interaction that is usually on the order of 10 meV–100 meV. These forces are generally stronger than the vdW dispersion. The angle-averaged Debye formula, describing this dipole–induced dipole interaction, is given by[60]

$$V_{\text{Debye}} = -\frac{\boldsymbol{d}_A^2 \tilde{\alpha}_B}{R^6}, \tag{16}$$

where A is the polar system and B is the non-polar system. This potential has the same R^{-6} behavior as the London formula in Eq. (13). In symmetry adapted perturbation theory,[72] this interaction is usually known as the induction term (E_{ind}).

The interaction between a polar water molecule and a non-polar benzene molecule is investigated here.[73] The complex is set in a configuration where the oxygen is pointing toward the benzene ring, as shown in the inset of Fig. 5. In this geometry, the interaction is dominated by the dipole–induced dipole forces and hydrogen bonding is minimal. The structures of the separate fragments are optimized using DFT/B3LYP with a 6-31+G** basis set.

TABLE II. Polarizability α_{yy} and mean polarizability $\bar{\alpha}$ for $(H_2)_2$ at bond distance 3.6 Å (obtained using finite differences). All quantities are in atomic units. The cavity frequency is $\omega = 12.7$ eV, and the induced effects reported for each field polarization are evaluated by subtracting the corresponding values without the cavity.

$(H_2)_2$	α_{xx}	α_{yy}	α_{zz}	$\bar{\alpha}$
CCSD	12.81	8.98	8.58	10.12
ε_x	−0.18	−0.05	−0.06	−0.10
ε_y	−0.09	−0.08	−0.06	−0.08
ε_z	−0.10	−0.02	−0.09	−0.07
DFT/OEP	12.14	9.16	8.83	10.13
ε_x	−0.11	−0.04	−0.04	−0.06
ε_y	−0.05	−0.13	−0.05	−0.08
ε_z	−0.05	−0.05	−0.12	−0.07

TABLE III. Polarizability α_{yy} and mean polarizability $\bar{\alpha}$ for H_2 (obtained using finite differences). All quantities are in atomic units. The cavity frequency is $\omega = 12.7$ eV, and the induced effects reported for each field polarization are evaluated by subtracting the corresponding values without the cavity.

H_2	α_{xx}	α_{yy}	α_{zz}	$\bar{\alpha}$
CCSD	6.53	4.34	4.34	5.07
ε_x	−0.08	−0.03	−0.03	−0.05
ε_y	−0.05	−0.04	−0.00	−0.03
ε_z	−0.05	−0.00	−0.04	−0.03
DFT/OEP	6.24	4.50	4.50	5.08
ε_x	−0.06	−0.02	−0.02	−0.03
ε_y	−0.03	−0.06	−0.03	−0.04
ε_z	−0.03	−0.03	−0.06	−0.04

In Fig. 5, we show the potential energy curves calculated using HF, CCSD, QED-HF, and QED-CCSD-1 with a 6-31+G* basis set. The field polarization is set along the dipole. We first note that HF and QED-HF are repulsive outside and inside the cavity. For CCSD, the weakly interacting complex has a metastable state with a barrier of 3 meV. Inside the cavity, instead, the QED-CCSD-1 potential energy curve becomes repulsive. The cavity-induced effect is here much larger (26 meV) than the observed effects for the H_2 dimer.

In Table IV, the dipole moment of H_2O and the polarizability of benzene, outside and inside the cavity, are shown. Inside the cavity, we see a small decrease (0.003 D) of the permanent

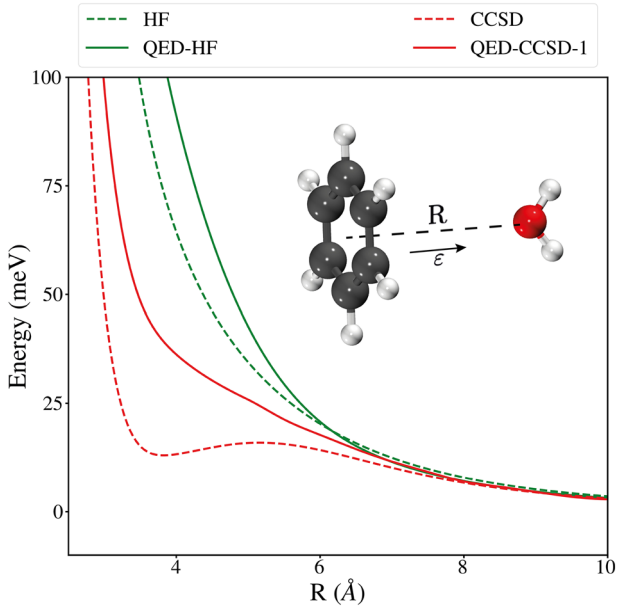

FIG. 5. Potential energy curve for the benzene–H_2O complex, both outside (dashed lines) and inside a cavity with cavity frequency $\omega = 13.6$ eV with field polarization along the dipole. Energies are relative to the energy of the isolated fragments.

TABLE IV. Dipole d for water and polarizability α parallel and perpendicular to d for benzene. Calculated outside and inside a cavity with field polarization along d and frequency ω = 13.6 eV.

Method	$\alpha_\perp$	$\alpha_\parallel$	$\bar{\alpha}$	d [D]
CCSD	78.55	40.83	65.97	2.304
QED-CCSD-1	77.60	33.23	62.81	2.301

dipole and a sizable reduction (7.60 a.u.) of the benzene polarizability along the polarization. A possible reason for the large cavity effect on $\alpha_\parallel$ could be connected to the aromaticity of benzene and its diffuse electrons. However, this requires further investigation.[74] Substituting the values in Table IV into Eq. (16), and comparing the size of the interaction outside and inside the cavity, we estimate a destabilization of 0.5 meV at R = 3.8 Å. This is much smaller than the corresponding destabilization observed in Fig. 5 of about 26 meV. This indicates that, as in the case of vdW, the purely electrostatic interaction model is not sufficient to describe the effect.

C. Hydrogen bonds

Hydrogen bonding arises when a hydrogen atom forms a bridge between two electronegative species.[75] A typical hydrogen bond energy is about 100 meV–300 meV and is one of the stronger intermolecular interactions. The electrostatic dipole–dipole energy is given by[61]

$$V_{\text{dipole}} = \frac{1}{R^3}\left(\boldsymbol{d}_A \cdot \boldsymbol{d}_B - \frac{3(\boldsymbol{d}_A \cdot \boldsymbol{R})(\boldsymbol{d}_B \cdot \boldsymbol{R})}{R^2}\right) \tag{17}$$

and represents the leading term in this interaction. However, it is now widely accepted that this kind of interaction is also characterized by a sizable charge transfer component, which contributes with a relatively large percentage (about 2 eV–3 eV per transferred electron) to the binding energy.[76,77]

Investigating hydrogen bonding is crucial to understand cavity-induced effects on the physical and chemical properties of solvents. In this section, we investigate the water dimer as a simple model for liquid water. For HF and CC calculations, we use an aug-cc-pVDZ basis set. The OEP calculations are performed using a spherical grid centered around each atom with radius 12 and spacing 0.28 a_0. The CCSD(T)/aug-cc-pVDZ equilibrium geometry is obtained from Ref. 77. The field polarization is chosen to be along the O–O direction, and the cavity frequency is set to the first CCSD excitation energy of water, ω = 7.86 eV.

In Fig. 6, we present the potential energy curve of the water dimer as a function of the O–O distance (R). In this case, the non-correlated methods (HF and DFT/OEP) capture the bond. Outside the cavity, DFT/OEP gives a slightly smaller binding energy than HF, and they both underestimate the energy compared to CCSD (214 meV). Inside the cavity, QED-CCSD-1 predicts a weaker hydrogen bond. The non-correlated methods (QED-HF and QEDFT/OEP) do not capture this cavity-induced destabilization of about 22 meV (10%), which indicates that the effect is due to correlation.

The electrostatic contribution to the binding energy can be estimated using the dipole moments shown in Table V and Eq. (17).

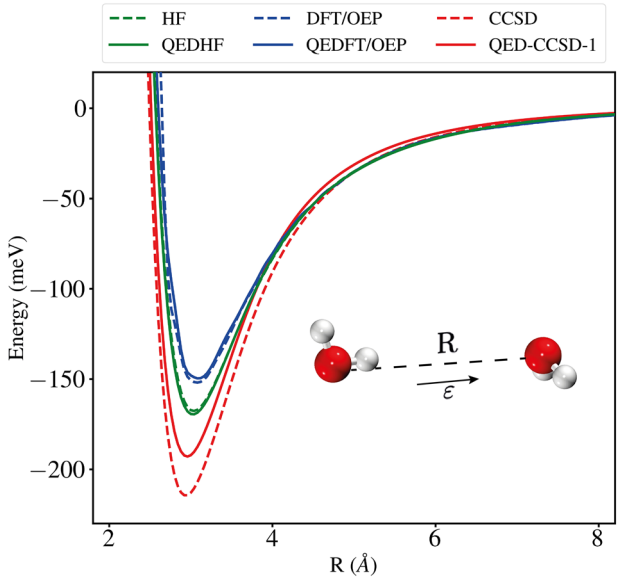

FIG. 6. Potential energy curves of $(H_2O)_2$ for different distances R between the oxygen atoms, outside (dashed) and inside a cavity (solid). The cavity polarization is along R with frequency ω = 7.86 eV. The structures of the water fragments are fixed.

The electrostatic treatment predicts a cavity-induced stabilization of about 0.2 meV, in contrast to the destabilization shown in Fig. 6. From this observation, it is clear that cavity-induced effects are not explained from a purely electrostatic picture.

As discussed above, hydrogen bonds are characterized by a relatively large charge transfer contribution. To investigate this aspect, we perform a charge displacement (CD) analysis[76,78] in Fig. 7. The charge displacement function $[\Delta q(z)]$ is defined from the density difference $\Delta\rho = \rho_{Dimer} - (\rho_{(H_2O)_A} + \rho_{(H_2O)_B})$ as

$$\Delta q(z) = \int_{-\infty}^{\infty}\int_{-\infty}^{\infty}\int_{-\infty}^{z} \Delta\rho(x,y,z')\,dx\,dy\,dz'. \tag{18}$$

This function quantitatively describes the amount of charge that has been moved along the z-direction. In particular, when Δq is positive, electrons are moved to the left, and they change direction when it is negative. For the water dimer outside the cavity, electrons are moved from the donor molecule (right) to the acceptor (left). A net charge transfer of about 10 me^- can be observed in the middle (dashed line) of the hydrogen bond. By placing the system inside the cavity, the

TABLE V. Dipole moments of isolated water fragments A and B, outside and inside the cavity. The field polarization is along the O–O direction and ω = 7.86 eV. In the hydrogen bond, A is the donor while B is the acceptor.

Method	d_A [D]	d_B [D]
CCSD	1.853	1.853
QED-CCSD-1	1.860	1.850
DFT/OEP	2.014	2.014
QEDFT/OEP	2.025	2.021

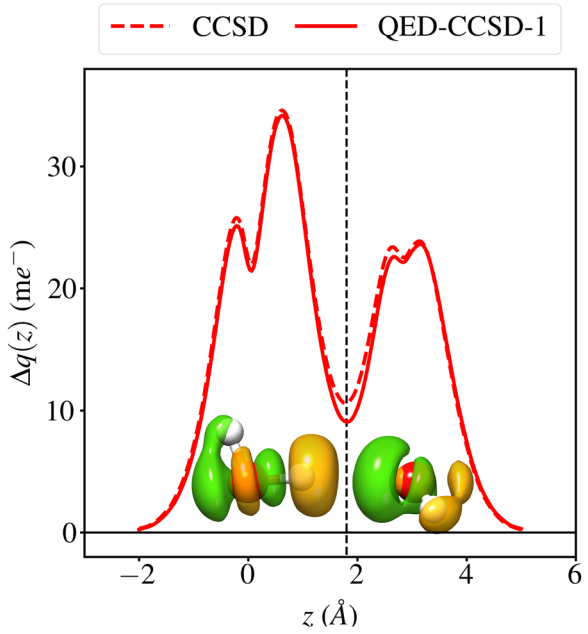

FIG. 7. CCSD and QED-CCSD-1 bond formation charge displacement analysis of $(H_2O)_2$ inside (solid) and outside (dashed) a cavity. The fragments are separated by 3.0 Å. The cavity polarization is along z.

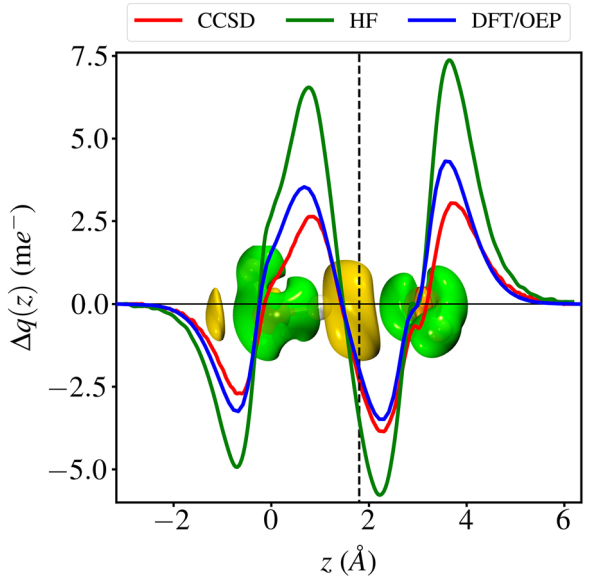

FIG. 8. Charge displacement analysis of the ground state cavity-induced density difference of $(H_2O)_2$. The fragments are separated by 3.0 Å. The cavity polarization is along z.

number of transferred electrons is reduced by about 2 me^-. This is in line with the weaker hydrogen bond observed in the potential energy curve and, following Ref. 76, it corresponds to a decrease of about 4 meV–6 meV in the binding energy.

In Fig. 8, the CD analysis has been applied to the ground state cavity-induced density difference ($\Delta\rho = \rho^{\mathrm{GS}}_{\mathrm{cav}} - \rho^{\mathrm{GS}}_{\mathrm{nocav}}$) calculated using HF, CCSD, and DFT/OEP. In this case, all methodologies show a qualitatively similar behavior and predict a reduction of charge transfer from donor to acceptor of about 2–3 me^- (extracted at the same position as in Fig. 7). The overall effect is a charge localization on the water fragments. The reduction of charge transfer for small distances is consistent with the observations of Ref. 25 and originates mainly from the DSE. From a more quantitative analysis, we see that Hartree–Fock overestimates the cavity-induced charge transfer compared to coupled cluster. On the other hand, the DFT/OEP curve is closer to the correlated result. In general, DFT is better equipped to describe the density than Hartree–Fock.[79]

D. Cavity-induced non-additive properties

Even when molecules are far away from each other inside a cavity, they still interact.[25] This results in non-additive properties of the dissociated system, e.g., the energy of the dissociated complex will not be equal to the sum of the energies of the individual fragments. In this section, we investigate these cavity-induced non-size-extensive properties of the QED Hamiltonian and their implications.

The main non-additive effect can be attributed to the DSE, which rewritten in terms of contributions from the individual fragments takes the form

$$E^{\mathrm{complex}}_{\mathrm{DSE}} = \sum_{n}^{N_f} E^{(n)}_{\mathrm{DSE}} + \lambda^2 \sum_{n<m}^{N_f} \langle (\boldsymbol{\varepsilon}\cdot\Delta\boldsymbol{d}^{(m)})(\boldsymbol{\varepsilon}\cdot\Delta\boldsymbol{d}^{(n)})\rangle, \tag{19}$$

where N_f is the number of fragments, $\Delta\boldsymbol{d} = \sum_n \Delta\boldsymbol{d}^{(n)}$, and $E^{(n)}_{\mathrm{DSE}}$ is the DSE for fragment n. The last term in Eq. (19) is the non-additive part. For identical fragments, the expression simplifies to

$$\Delta\mathcal{E}_{\mathrm{DSE}} = \frac{\lambda^2}{2}\langle (\boldsymbol{\varepsilon}\cdot\Delta\boldsymbol{d}^{(1)})(\boldsymbol{\varepsilon}\cdot\Delta\boldsymbol{d}^{(2)})\rangle (N_f^2 - N_f), \tag{20}$$

showing explicitly that the effect is quadratic with the number of fragments. In Eq. (20), $\Delta\boldsymbol{d}^{(1)}$ and $\Delta\boldsymbol{d}^{(2)}$ are the dipole fluctuations of two equivalent fragments. The bilinear term will also contribute,

$$E^{\mathrm{complex}}_{\mathrm{BI}} = \lambda\sqrt{\frac{\omega}{2}}\sum_{n}^{N_f}\langle (b+b^\dagger)(\boldsymbol{\varepsilon}\cdot\Delta\boldsymbol{d}^{(n)})\rangle, \tag{21}$$

although we expect the contribution to be smaller.

In Fig. 9, we analyze the non-additive part of the total energy $[\Delta\mathcal{E} = E^{\mathrm{complex}} - \sum_n E^{(n)}]$ for water molecules separated by 200 Å (see the inset of Fig. 9) using a 6-31G basis set. The properties of the QED Hamiltonian make the total energy non-additive, and the QED-CC approach is able to capture this behavior (black dashed line). In the limit $\lambda \to 0$, the QED-CC approach is size-extensive as for standard coupled cluster theory for electrons. On the other hand, QED-HF always has size-extensive solutions and fails to describe the non-additive nature of the cavity interaction (blue dashed lines).

We observe a quadratic scaling of the non-additive part with respect to the number of fragments, as expected from Eq. (20). The

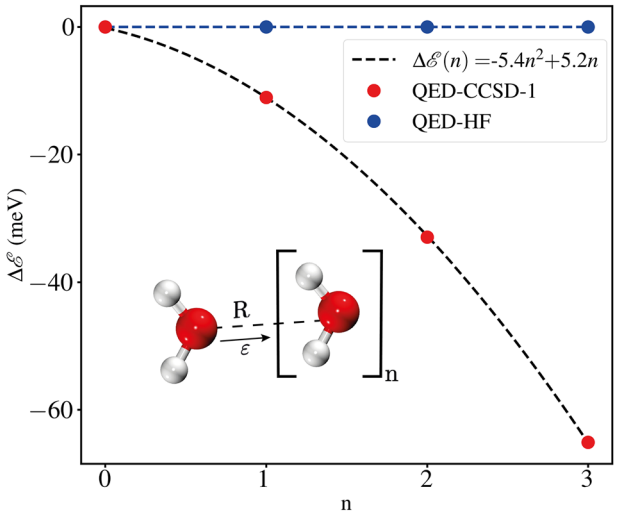

FIG. 9. The non-additive part of the total energy, $\Delta\mathcal{E} = \mathrm{E}_{(\mathrm{H_2O})_{n+1}} - (n+1)\mathrm{E}_{\mathrm{H_2O}}$ of $(H_2O)_{n+1}$. Fragments are separated by 200 Å and placed inside a cavity with ω = 7.86 eV. The fitted curve has $\mathcal{R}^2 > 0.999$.

fit of the data (dashed black line) highlights also a small deviation (0.2) in the linear term, likely due to the bilinear correction described in Eq. (21). This result implies that the collective ground state interaction between many molecules could be observable experimentally, if enough molecules are considered. We point out that this effect is not limited by the dipole approximation since we consider a stretching of the coordinates in a direction that is parallel to the field polarization (perpendicular to the wave vector $\boldsymbol{k}$). This non-additive effect could be very interesting in solvation environments, where a solute can interact with a large number of solvent molecules through the field.

IV. CONCLUSIONS

Using available QED *ab initio* methodologies, we investigated cavity-induced effects on intermolecular interactions. Four types of interactions have been studied: van der Waals forces, induction interactions, hydrogen bonding, and cavity mediated long-range interactions. In all cases, correlation is deemed crucial to describe the systems. Several effects of the cavity seem rather counter-intuitive from a chemical point of view. The van der Waals forces between two non-polar molecules behave as R^{-6}. However, inside the cavity, an additional R^{-3} component originates from electron–photon correlation, usually characteristic of a dipole–dipole interaction. For the induction interaction and hydrogen bonding, the cavity-induced effect is larger than for the van der Waals. In both cases, the binding energy and polarizability are reduced. We also demonstrate that, inside the cavity, molecules remain permanently correlated at arbitrary distances.

Our results suggest that cavity fields can be used to modify the ground state interactions in intermolecular systems. This opens possibilities for novel applications in several fields, ranging from the control of solvent assisted reactions to modifying higher-order structures in biological macromolecules. These results could prove useful in understanding future experiments in polaritonic chemistry.

SUPPLEMENTARY MATERIAL

See the supplementary material for additional results for the $(H_2)_2$ molecule in an optical cavity with different polarization directions, study of the cavity frequency effects on the binding energy of $(H_2)_2$ and water dimer, and analysis of cavity-induced effects on the $(H_2)_2$ molecule in a C_{2v} configuration.

ACKNOWLEDGMENTS

T.S.H. and H.K. acknowledge computing resources through UNINETT Sigma2—the National Infrastructure for High Performance Computing and Data Storage in Norway, through Project No. NN2962k. T.S.H. and H.K. acknowledge funding from the Marie Skłodowska-Curie European Training Network "COSINE—COmputational Spectroscopy In Natural sciences and Engineering," Grant Agreement No. 765739, the Research Council of Norway through FRINATEK Project Nos. 263110 and 275506. C.S. and A.R. acknowledge support of the RouTe Project (Grant No. 13N14839), financed by the Federal Ministry of Education and Research [Bundesministerium für Bildung und Forschung (BMBF)], the European Research Council (Grant No. ERC-2015-AdG694097), the Cluster of Excellence "Advanced Imaging of Matter" (AIM), and Grupos Consolidados (Grant No. IT1249-19). The Flatiron Institute is a division of the Simons Foundation.

DATA AVAILABILITY

The data that support the findings of this study are available within the article and its supplementary material.

REFERENCES

[1] P. Atkins and J. de Paula, *Physical Chemistry* (OUP Oxford, 2016).
[2] C. Heald and H. W. Thompson, "Intermolecular forces and solvent effects. III," Proc. R. Soc. London, Ser. A **268**, 89–99 (1962).
[3] J. M. Garver, Y.-R. Fang, N. Eyet, S. M. Villano, V. M. Bierbaum, and K. C. Westaway, "A direct comparison of reactivity and mechanism in the gas phase and in solution," J. Am. Chem. Soc. **132**, 3808–3814 (2010).
[4] D. L. Nelson and M. M. Cox, *Lehninger Principles of Biochemistry*, 6th ed. (Macmillan, 2012).
[5] Y. Cao, V. Fatemi, S. Fang, K. Watanabe, T. Taniguchi, E. Kaxiras, and P. Jarillo-Herrero, "Unconventional superconductivity in magic-angle graphene superlattices," Nature **556**, 43–50 (2018).
[6] A. Kerelsky, L. J. McGilly, D. M. Kennes, L. Xian, M. Yankowitz, S. Chen, K. Watanabe, T. Taniguchi, J. Hone, C. Dean, A. Rubio, and A. N. Pasupathy, "Maximized electron interactions at the magic angle in twisted bilayer graphene," Nature **572**, 95–100 (2019).
[7] H. M. Hill, "Twisted bilayer graphene enters a new phase," Phys. Today **73**(1), 18 (2020).
[8] L. Xian, D. M. Kennes, N. Tancogne-Dejean, M. Altarelli, and A. Rubio, "Multiflat bands and strong correlations in twisted bilayer boron nitride: Doping-induced correlated insulator and superconductor," Nano Lett. **19**, 4934–4940 (2019).
[9] J. A. Hutchison, T. Schwartz, C. Genet, E. Devaux, and T. W. Ebbesen, "Modifying chemical landscapes by coupling to vacuum fields," Angew. Chem., Int. Ed. **51**, 1592–1596 (2012).

[10]A. Thomas, J. George, A. Shalabney, M. Dryzhakov, S. J. Varma, J. Moran, T. Chervy, X. Zhong, E. Devaux, C. Genet *et al.*, "Ground-state chemical reactivity under vibrational coupling to the vacuum electromagnetic field," Angew. Chem., Int. Ed. **128**, 11634–11638 (2016).
[11]B. Munkhbat, M. Wersäll, D. G. Baranov, T. J. Antosiewicz, and T. Shegai, "Suppression of photo-oxidation of organic chromophores by strong coupling to plasmonic nanoantennas," Sci. Adv. **4**, eaas9552 (2018).
[12]A. Thomas, L. Lethuillier-Karl, K. Nagarajan, R. M. A. Vergauwe, J. George, T. Chervy, A. Shalabney, E. Devaux, C. Genet, J. Moran, and T. W. Ebbesen, "Tilting a ground-state reactivity landscape by vibrational strong coupling," Science **363**, 615–619 (2019).
[13]H. Hiura, A. Shalabney, and J. George, "Vacuum-field catalysis: Accelerated reactions by vibrational ultra strong coupling," chemRxiv:7234721.v4 (2018).
[14]J. Lather, P. Bhatt, A. Thomas, T. W. Ebbesen, and J. George, "Cavity catalysis by cooperative vibrational strong coupling of reactant and solvent molecules," Angew. Chem., Int. Ed. **58**, 10635–10638 (2019).
[15]F. Herrera and F. C. Spano, "Cavity-controlled chemistry in molecular ensembles," Phys. Rev. Lett. **116**, 238301 (2016).
[16]J. A. Campos-Gonzalez-Angulo, R. F. Ribeiro, and J. Yuen-Zhou, "Resonant catalysis of thermally activated chemical reactions with vibrational polaritons," Nat. Commun. **10**, 4685 (2019).
[17]V. M. Agranovich, M. Litinskaia, and D. G. Lidzey, "Cavity polaritons in microcavities containing disordered organic semiconductors," Phys. Rev. B **67**, 085311 (2003).
[18]D. Wang, H. Kelkar, D. Martin-Cano, T. Utikal, S. Götzinger, and V. Sandoghdar, "Coherent coupling of a single molecule to a scanning Fabry-Perot microcavity," Phys. Rev. X **7**, 021014 (2017).
[19]O. S. Ojambati, R. Chikkaraddy, W. D. Deacon, M. Horton, D. Kos, V. A. Turek, U. F. Keyser, and J. J. Baumberg, "Quantum electrodynamics at room temperature coupling a single vibrating molecule with a plasmonic nanocavity," Nat. Commun. **10**, 1049 (2019).
[20]M. Wersäll, J. Cuadra, T. J. Antosiewicz, S. Balci, and T. Shegai, "Observation of mode splitting in photoluminescence of individual plasmonic nanoparticles strongly coupled to molecular excitons," Nano Lett. **17**, 551–558 (2017).
[21]E. Orgiu, J. George, J. A. Hutchison, E. Devaux, J. F. Dayen, B. Doudin, F. Stellacci, C. Genet, J. Schachenmayer, C. Genes, G. Pupillo, P. Samorì, and T. W. Ebbesen, "Conductivity in organic semiconductors hybridized with the vacuum field," Nat. Mater. **14**, 1123–1129 (2015).
[22]X. Zhong, T. Chervy, L. Zhang, A. Thomas, J. George, C. Genet, J. A. Hutchison, and T. W. Ebbesen, "Energy transfer between spatially separated entangled molecules," Angew. Chem., Int. Ed. **56**, 9034–9038 (2017).
[23]D. Hagenmüller, J. Schachenmayer, S. Schütz, C. Genes, and G. Pupillo, "Cavity-enhanced transport of charge," Phys. Rev. Lett. **119**, 223601 (2017).
[24]R. Sáez-Blázquez, J. Feist, A. I. Fernández-Domínguez, and F. J. García-Vidal, "Organic polaritons enable local vibrations to drive long-range energy transfer," Phys. Rev. B **97**, 241407 (2018).
[25]C. Schäfer, M. Ruggenthaler, H. Appel, and A. Rubio, "Modification of excitation and charge transfer in cavity quantum-electrodynamical chemistry," Proc. Natl. Acad. Sci. U. S. A. **116**, 4883–4892 (2019).
[26]G. Groenhof, C. Climent, J. Feist, D. Morozov, and J. J. Toppari, "Tracking polariton relaxation with multiscale molecular dynamics simulations," J. Phys. Chem. Lett. **10**, 5476–5483 (2019).
[27]M. Hertzog, M. Wang, J. Mony, and K. Börjesson, "Strong light–matter interactions: A new direction within chemistry," Chem. Soc. Rev. **48**, 937–961 (2019).
[28]H. Hübener, U. De Giovannini, C. Schäfer, J. Andberger, M. Ruggenthaler, J. Faist, and A. Rubio, "Engineering quantum materials with chiral optical cavities," Nat. Mater. (2020).
[29]A. Thomas, E. Devaux, K. Nagarajan, T. Chervy, M. Seidel, D. Hagenmüller, S. Schütz, J. Schachenmayer, C. Genet, G. Pupillo, and T. W. Ebbesen, "Exploring superconductivity under strong coupling with the vacuum electromagnetic field," arXiv:1911.01459 (2019).
[30]M. A. Sentef, M. Ruggenthaler, and A. Rubio, "Cavity quantum-electrodynamical polaritonically enhanced electron-phonon coupling and its influence on superconductivity," Sci. Adv. **4**, eaau6969 (2018).
[31]F. Schlawin, A. Cavalleri, and D. Jaksch, "Cavity-mediated electron-photon superconductivity," Phys. Rev. Lett. **122**, 133602 (2019).
[32]R. H. Dicke, "Coherence in spontaneous radiation processes," Phys. Rev. **93**, 99–110 (1954).
[33]E. T. Jaynes and F. W. Cummings, "Comparison of quantum and semiclassical radiation theories with application to the beam maser," Proc. IEEE **51**, 89–109 (1963).
[34]F. W. Cummings, "Stimulated emission of radiation in a single mode," Phys. Rev. **140**, A1051–A1056 (1965).
[35]T. Anoop, L. Lethuillier-Karl, J. Moran, and T. Ebbesen, "Comment on 'On the SN_2 reactions modified in vibrational strong coupling experiments: Reaction mechanisms and vibrational mode assignments'," chemRxiv:12982358 (2020).
[36]J. Galego, C. Climent, F. J. Garcia-Vidal, and J. Feist, "Cavity Casimir-Polder forces and their effects in ground-state chemical reactivity," Phys. Rev. X **9**, 021057 (2019).
[37]F. Herrera, "Photochemistry with quantum optics from a non-adiabatic quantum trajectory perspective," Chem **6**, 7–9 (2020).
[38]X. Li, A. Mandal, and P. Huo, "Resonance theory of vibrational strong couplings in polariton chemistry," chemrxiv.12915701.v1 (2020).
[39]I. Vurgaftman, B. S. Simpkins, A. D. Dunkelberger, and J. C. Owrutsky, "Negligible effect of vibrational polaritons on chemical reaction rates via the density of states pathway," J. Phys. Chem. Lett. **11**, 3557–3562 (2020).
[40]B. W. Shore and P. L. Knight, "The Jaynes-Cummings model," J. Mod. Opt. **40**, 1195–1238 (1993).
[41]M. Ruggenthaler, J. Flick, C. Pellegrini, H. Appel, I. V. Tokatly, and A. Rubio, "Quantum-electrodynamical density-functional theory: Bridging quantum optics and electronic-structure theory," Phys. Rev. A **90**, 012508 (2014).
[42]T. S. Haugland, E. Ronca, E. F. Kjønstad, A. Rubio, and H. Koch, "Coupled cluster theory for molecular polaritons: Changing ground and excited states," Phys. Rev. X **10**, 041043 (2020).
[43]J. Flick, C. Schäfer, M. Ruggenthaler, H. Appel, and A. Rubio, "Ab initio optimized effective potentials for real molecules in optical cavities: Photon contributions to the molecular ground state," ACS Photonics **5**, 992–1005 (2018).
[44]S. Latini, D. Shin, S. A. Sato, C. Schäfer, U. D. Giovannini, H. Hübener, and A. Rubio, "The ferroelectric photo-groundstate of $SrTiO_3$: Cavity materials engineering," arXiv:2101.11313 (2021).
[45]E. A. DePrince, "Cavity-modulated ionization potentials and electron affinities from quantum electrodynamics coupled-cluster theory," arXiv:2011.12768 (2020).
[46]D. Sidler, C. Schäfer, M. Ruggenthaler, and A. Rubio, "Polaritonic chemistry: Collective strong coupling implies strong local modification of chemical properties," J. Phys. Chem. Lett. **12**, 508–516 (2021).
[47]S. Grimme, "Density functional theory with London dispersion corrections," WIREs Comput. Mol. Sci. **1**, 211–228 (2011).
[48]H. Spohn, *Dynamics of Charged Particles and Their Radiation Field* (Cambridge University Press, 2004).
[49]C. Cohen-Tannoudji, J. Dupont-Roc, and G. Grynberg, *Photons and Atoms: Introduction to Quantum Electrodynamics* (Wiley-VCH, 1997).
[50]E. A. Power and S. Zienau, "Coulomb gauge in non-relativistic quantum electrodynamics and the shape of spectral lines," Proc. R. Soc. London, Ser. A **251**, 427–454 (1959).
[51]C. Schäfer, M. Ruggenthaler, V. Rokaj, and A. Rubio, "Relevance of the quadratic diamagnetic and self-polarization terms in cavity quantum electrodynamics," ACS Photonics **7**, 975–990 (2020).
[52]T. Helgaker, P. Jørgensen, and J. Olsen, *Molecular Electronic-Structure Theory* (John Wiley & Sons, Ltd., Chichester, UK, 2000).
[53]R. G. Parr and W. Yang, *Density-Functional Theory of Atoms and Molecules* (Oxford Science Publications, 1989).
[54]S. D. Folkestad, E. F. Kjønstad, R. H. Myhre, J. H. Andersen, A. Balbi, S. Coriani, T. Giovannini, L. Goletto, T. S. Haugland, A. Hutcheson, I.-M. Høyvik, T. Moitra, A. C. Paul, M. Scavino, A. S. Skeidsvoll, Å. H. Tveten, and H. Koch, "e^T 1.0: An open source electronic structure program with emphasis on coupled cluster and multilevel methods," J. Chem. Phys. **152**, 184103 (2020).
[55]P. Hohenberg and W. Kohn, "Inhomogeneous electron gas," Phys. Rev. **136**, B864–B871 (1964).

[56]W. Kohn and L. J. Sham, "Self-consistent equations including exchange and correlation effects," Phys. Rev. **140**, A1133–A1138 (1965).
[57]S. Kümmel and J. P. Perdew, "Optimized effective potential made simple: Orbital functionals, orbital shifts, and the exact Kohn-Sham exchange potential," Phys. Rev. B **68**, 035103 (2003).
[58]C. Pellegrini, J. Flick, I. V. Tokatly, H. Appel, and A. Rubio, "Optimized effective potential for quantum electrodynamical time-dependent density functional theory," Phys. Rev. Lett. **115**, 093001 (2015).
[59]N. Tancogne-Dejean, M. J. T. Oliveira, X. Andrade, H. Appel, C. H. Borca, G. Le Breton, F. Buchholz, A. Castro, S. Corni, A. A. Correa *et al.*, "Octopus, a computational framework for exploring light-driven phenomena and quantum dynamics in extended and finite systems," J. Chem. Phys. **152**, 124119 (2020).
[60]P. Atkins and R. Friedman, *Molecular Quantum Mechanics* (OUP Oxford, 2011).
[61]D. P. Craig and T. Thirunamachandranm, *Molecular Quantum Electrodynamics: An Introduction to Radiation-Molecule* (Dover Publications, Inc., Mineola, NY, 1984).
[62]S. Y. Buhmann, *Dispersion Forces I: Macroscopic Quantum Electrodynamics and Ground-State Casimir, Casimir–Polder and van der Waals Forces* (Springer, 2013), Vol. 247.
[63]S. Buhmann, *Dispersion Forces II: Many-Body Effects, Excited Atoms, Finite Temperature and Quantum Friction* (Springer, 2013), Vol. 248.
[64]A. Salam, *Non-Relativistic QED Theory of the van der Waals Dispersion Interaction* (Springer, 2016).
[65]C. Schäfer, M. Ruggenthaler, and A. Rubio, "Ab initio nonrelativistic quantum electrodynamics: Bridging quantum chemistry and quantum optics from weak to strong coupling," Phys. Rev. A **98**, 043801 (2018).
[66]R. Chikkaraddy, B. De Nijs, F. Benz, S. J. Barrow, O. A. Scherman, E. Rosta, A. Demetriadou, P. Fox, O. Hess, and J. J. Baumberg, "Single-molecule strong coupling at room temperature in plasmonic nanocavities," Nature **535**, 127–130 (2016).
[67]S. De Liberato, "Virtual photons in the ground state of a dissipative system," Nat. Commun. **8**, 1465 (2017).
[68]F. London, "The general theory of molecular forces," Trans. Faraday Soc. **33**, 8b–26 (1937).
[69]H. Koch, O. Christiansen, P. Jørgensen, A. M. Sanchez de Merás, and T. Helgaker, "The CC3 model: An iterative coupled cluster approach including connected triples," J. Chem. Phys. **106**, 1808–1818 (1997).
[70]M. Urban, J. Noga, S. J. Cole, and R. J. Bartlett, "Towards a full CCSDT model for electron correlation," J. Chem. Phys. **83**, 4041–4046 (1985).
[71]E. A. Power and T. Thirunamachandran, "Quantum electrodynamics in a cavity," Phys. Rev. A **25**, 2473 (1982).
[72]K. Patkowski, "Recent developments in symmetry-adapted perturbation theory," WIREs Comput. Mol. Sci. **10**, e1452 (2020).
[73]M. Prakash, K. G. Samy, and V. Subramanian, "Benzene–water (BZW_n (n = 1–10)) clusters," J. Phys. Chem. A **113**, 13845–13852 (2009).
[74]P. Lazzeretti, "Assessment of aromaticity via molecular response properties," Phys. Chem. Chem. Phys. **6**, 217–223 (2004).
[75]E. Arunan, G. R. Desiraju, R. A. Klein, J. Sadlej, S. Scheiner, I. Alkorta, D. C. Clary, R. H. Crabtree, J. J. Dannenberg, P. Hobza, H. G. Kjaergaard, A. C. Legon, B. Mennucci, and D. J. Nesbitt, "Definition of the hydrogen bond (IUPAC recommendations 2011)," Pure Appl. Chem. **83**, 1637–1641 (2011).
[76]D. Cappelletti, E. Ronca, L. Belpassi, F. Tarantelli, and F. Pirani, "Revealing charge-transfer effects in gas-phase water chemistry," Acc. Chem. Res. **45**, 1571–1580 (2012).
[77]E. Ronca, L. Belpassi, and F. Tarantelli, "A quantitative view of charge transfer in the hydrogen bond: The water dimer case," ChemPhysChem **15**, 2682–2687 (2014).
[78]L. Belpassi, I. Infante, F. Tarantelli, and L. Visscher, "The chemical bond between Au(I) and the noble gases. Comparative study of NgAuF and $NgAu^+$ (Ng = Ar, Kr, Xe) by density functional and coupled cluster methods," J. Am. Chem. Soc. **130**, 1048–1060 (2008).
[79]S. Kümmel and L. Kronik, "Orbital-dependent density functionals: Theory and applications," Rev. Mod. Phys. **80**, 3 (2008).